III. Results and Discussion

1. Histological findings in the coronary artery

Twenty-four swine had surgical treatments performed in two of the coronary arteries, LAD as well as either the LCX or RCA. A total of seventy-two arteries were treated as follows: 6 arteries received balloon angioplasty instead of the inflation of the delivery angioplasty, 6 arteries only treated with balloon angioplasty, 12 arteries were subjected to the intracoronary β-radiation ^{188}Re liquid-filled balloon (14 Gy, n = 6; 20 Gy, n = 6) following balloon injury, 6 arteries were subjected to the placement and inflation of the delivery balloon with sterile water instead of ^{188}Re following balloon injury, 6 arteries received the balloon-overstretch injury prior to intracoronary radiation, and 6 arteries received the balloon-overstretch injury after intracoronary radiation. One animal died during follow-up angioplasty. Histopathological examination of the coronary arteries revealed the occlusion by partially organized thrombosis accompanied with fibrocellular neotima and was observed in the sham control group, PTCA group, PTCA/Re group, and Re/PTCA group. Histomorphometric data were obtained from vessels that exhibited complete medial fracture (24 of 30 vessels), including the sham control group, PTCA group, Re188 group, PTCA/Re group and Re/PTCA group. Animals were scarified and coronary arteries were isolated to detect gene expression at 1 day and analyze the histopathology at 6 weeks after surgical treatments. Histopathologic analysis was performed in the LAD, LCX and RAC at 6 weeks. Re188 group included 3 LAD, and 3 RAC arteries. There were 3 LAD, and 3 RAC segments studied in the low-dose radiation group. There were 3 LAD and 3 RAC segments studied in the high-dose radiation group. The ^{188}Re solution activity was nearly 35 mCi/ml.

Of the 76 injured segments, most of them had obviously the phenomenon of restenosis in the vessel, one had the thrombosis, and two had no difference.

1-1. Histopathologic analysis

In the sham control group and the radiation only group at 20 Gy, coronary arteries had qualitatively similar histology. In coronary arteries of the sham control group, there were no neointimal proliferation, and no detectable lumen loss (Figure 8A). This finding was similar to the response in which the vessel was treated by 20 Gy-irradiation (data not shown). There was the reduction of neointima and evidence of thinned vessel wall despite equivalent IEL rupture with the treatment of 20 Gy-irradiation. However, in balloon-injured coronary arteries, at the site of IEL rupture and the intervening space filled with the neointimal formation, there was a maximal proliferation of SMCs migrating from the media to the intima and formed neointimal area observed by H&E staining (Figure 8D). In addition, the neointimal area in both groups, angioplasty prior to and after brachytherapy (PTCA/Re and Re/PTCA, respectively), was markedly smaller than that in the PTCA only group (PTCA only) (Figure 8B and 8C). Therefore, balloon overdilation was associated with the significant vascular injury and marked neointimal proliferation. Brachytherapy in injured site of coronary arteries can alleviate the damage and prevent the restenosis in Figure 8.

1-2. Histomorphmetry

In normal coronary arteries without the balloon injury and radiation exposure, the lumen area was 2250 ± 300 μm^2. However, the lumen area was 480 ± 150 μm^2 in the PTCA group (Table 9). The lumen area of coronary arteries in response to angioplasty prior to and after brachytherapy was greater than that in the treatment with PTCA alone. The lumen areas were 1100 ± 200 and 1300 ± 180 μm^2, respectively ($p < 0.01$ vs. PTCA alone). Therefore, the lumen area was increased by radiation following or after balloon injury. Significant reductions of the neointimal area were also observed in the angioplasty prior to and after brachytherapy (450 ± 130 μm^2 and 550 ± 200 μm^2 compared with 1200 ± 300 μm^2 for PTCA

treatment alone, $p < 0.01$) (Table 9). Therefore, radiation in injured site of coronary arteries can prevent the restenosis, and increase lumen area and decrease neointimal area

The lumen area was 1350 ± 280 μm^2 at low dose irradiation and 1100 ± 200 μm^2 at high dose irradiation. The exposure of radiation at 14 Gy was better increase of lumen area than that at 20 Gy in the model of porcine coronary artery ($p < 0.05$). Besides, there was an improved histological percent of neointimal formation in exposure to radiation at the dose of either 14 Gy or 20 Gy from ^{188}Re liquid-filled balloons. In our study, the exposure of radiation at 20 Gy was better reduction of neointimal formation than that at 14 Gy in the model of porcine coronary artery in Table 10. The neointimal area was 650 ± 120 μm^2 at low dose irradiation and 450 ± 130 μm^2 at high dose irradiation ($p < 0.05$). Therefore, in our data there were markedly increased lumen and decreased neointimal area at either 14 or 20 Gy (data not shown) following balloon injury and it seems that the radiated arteries had qualitatively greater responses at high dose irradiation than radiation-treated arteries at low dose irradiation in neointimal formation.

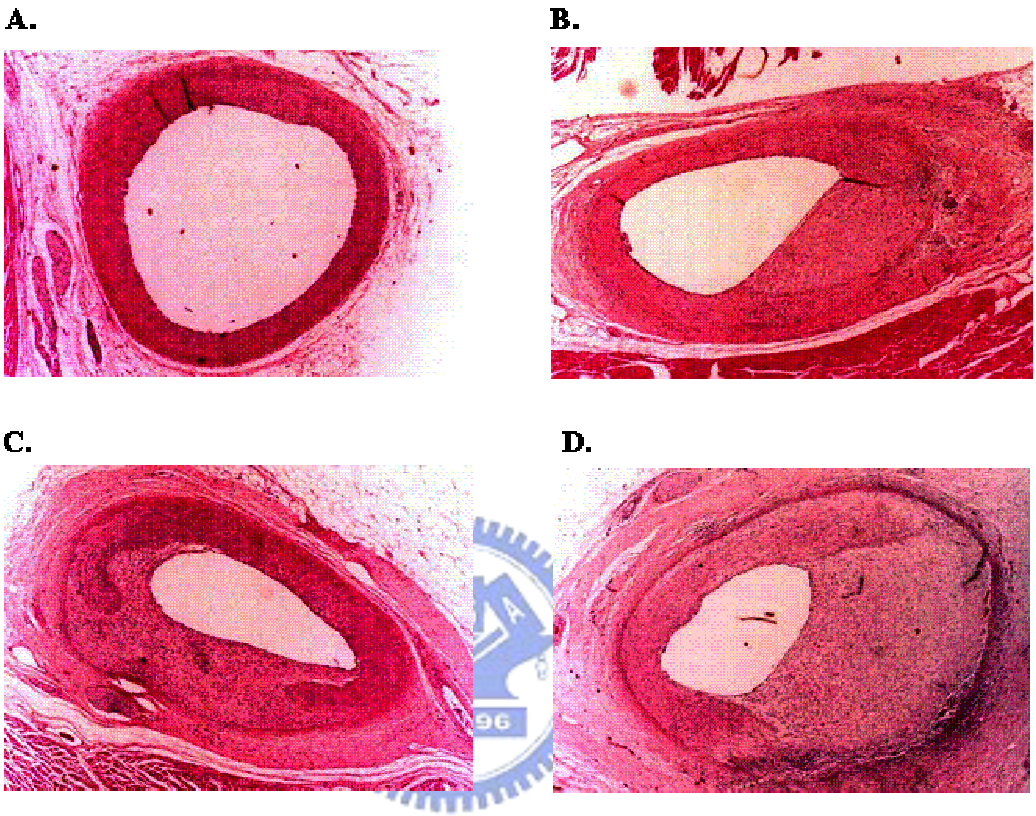

Figure 8. Porcine coronary arteries were subjected to angioplasty and/or brachytherapy at the dose of 20 Gy. The animals were sacrificed at 6 weeks later after balloon injury. Sections of perfusion-fixed arteries were analyzed by H&E staining described in "Materials and Methods." (A) Normal coronary arteries (sham control group), (B) coronary arteries with the treatment of angioplasty prior to brachtherapy (PTCA/Re group), (C) coronary arteries in response to brachtherapy prior to angioplasty (Re188/PTCA group), and (D) coronary arteries received PTCA alone (PTCA group) were observed by an optical microscope.

Table 9. Histomorphological assessment of porcine coronary arteries after surgical treatments.

Groups	Sham control	PTCA only	PTCA/Re	Re/PTCA
Number of arteries	**6**	**6**	**6**	**6**
Lumen area (μm^2)	2250 ± 300	480 ± 150	1100 ± 200	1300 ± 180
Neointimal area (μm^2)	90 ± 20	1200 ± 300	450 ± 130	550 ± 200

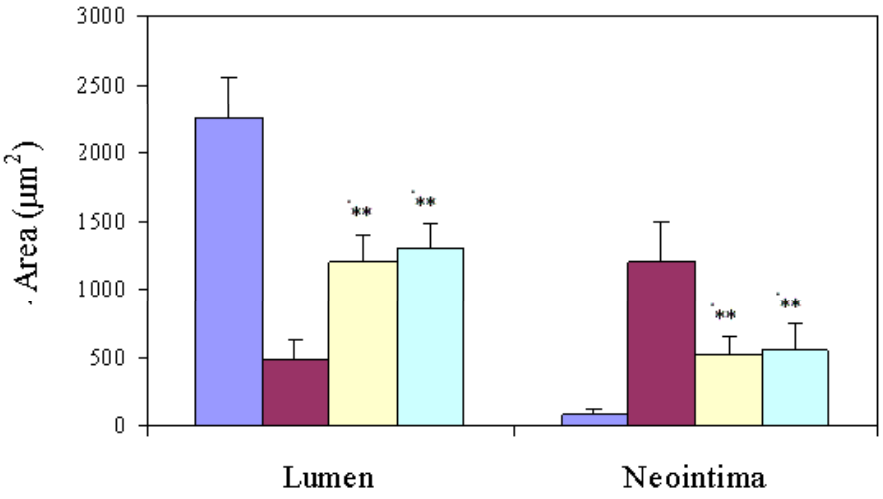

Figure 9. Histomorphology of coronary arteries in the effect in neointima and lumen. Each column is the mean ± SD of triplicate determinations. ** indicates $p < 0.01$ compared with injured arteries in PTCA group. Blue color responses the sham control group, brown color responses the PTCA only group, yellow responses the PTCA/Re group, and green responses the Re/PTCA group (20 Gy).

Table 10. Histomorphological assessment of porcine coronary arteries in response to radiation at 14 and 20 Gy.

Groups	Radiation dose, Gy		*p* value
	14	20	
Number of arteries	6	6	
Lumen area (μm^2)	1350 ± 280	1100 ± 200	0.032
Neointimal area (μm^2)	650 ± 120	450 ± 130	0.028

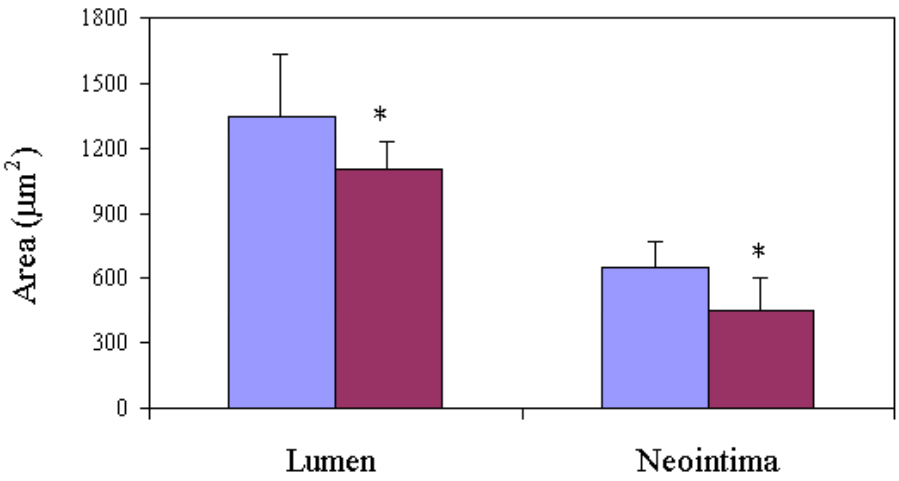

Figure 10. Histomorphology of coronary arteries in the effect in neointima and lumen exposed to radiation. * indicates that is significantly different between 20 Gy and 14 Gy radiated arteries determined by t test at $p < 0.05$. Blue color indicates 14 Gy-radiation and brown color indicates 20 Gy-radiation.

2. mRNA expression levels of adhesion molecule in vivo

The number of amplification cycles necessary to yield detectable PCR products and remain in the linear range of amplification was determined for each product and the minimal number of cycles necessary to yield sufficient product for analysis was used. The optimal number of PCR cycles for human GAPDH and NF-κB was determined to be 20 and 28, respectively. However, the number of cycles which was in 20 cycles for porcine GAPDH, 28 cycles for ICAM-1, 24 cycles for VCAM-1 was used (data not shown). The linearity of amplification was preserved for at least two additional cycles.

Functional importance in the inflammatory response of ICAM-1, and VCAM-1 expression by endothelial cells had recently been shown in the injured tissue. These molecules were involved in the adhesion of $CD34^+$ cells to endothelial cells and in the infiltrated migration of $CD34^+$ cells presented in previous studies. We investigated whether irradiation modifies the expression of these adhesion molecules in coronary arterial cells. Coronary artery is primarily composed of SMCs which play a vital role in neointimal formation. In Figure 11A, the expression of ICAM-1 significantly increased in PTCA only, PTCA/Re, and Re/PTCA groups ($p < 0.001$), all compared to the sham control group, but had no significant different in Re188 only group, compared to the sham control group. The expression of ICAM-1 was 2 folds higher in the PTCA only, PTCA/Re and Re/PTCA group than that in the sham control group. This increased expression was detected at 1 day after the post-treatments. Therefore, PTCA treatment might lead to increase the expression of ICAM-1, whereas there were not significantly different between PTCA/Re and Re/PTCA group, compared to PTCA only group. It showed whether PTCA was used before or after radiation, the expression of ICAM-1 was similar to the PTCA treatment only group. Balloon-overstretch injury prior to and after intracoronary radiation leaded to the same contribution of ICAM-1 expression. By contrast, ICAM-1 expression in Re188 group

significantly decreased compared with that in the balloon-injured group, in PTCA/Re, and Re/PTCA groups ($p < 0.001$). As a result, it represented that balloon-overstretch injury contributed to increase ICAM-1 expression not intracoronary radiation. Meanwhile, the mRNA of ICAM-1 in Re188 group was slightly increased compared with that in the sham control group but with no statistical significance. Therefore, intracoronary radiation alone did not cause the effect of ICAM-1 expression. Figure 12 showed the expression of ICAM-1 in porcine LAD and RCA. The expression of ICAM-1 was no statistical difference between LAD and RCA.

The mRNA of VCAM-1 of other post-treatments was significantly decreased compared with that of sham control arteries. Sham control arteries had a high expression of cell surface VCAM-1 in Figure 11B, which was approximately downregulated 1.5-fold when arteries were treated with angioplasty in PTCA, and Re/PTCA groups ($p < 0.01$). The expression of VCAM-1 was downregulated 2-fold in the PTCA/Re group ($p < 0.001$). It represented that balloon-overstretch injury resulted in the inhibition of VCAM-1 expression in the porcine model in our study. However, the mRNA of VCAM-1 in the PTCA/Re group was slightly decreased compared with that in the PTCA and Re/PTCA groups but with no statistical significance. Balloon-overstretch injury prior to and after intracoronary radiation caused the same contribution of VCAM-1 expression. By contrast, VCAM-1 expression in Re188 group slightly decreased compared with that in the PTCA group, in PTCA/Re, and Re/PTCA groups but no significant difference. Irradiation at the dose of 20 Gy induced a significant decrease of VCAM-1 ($p < 0.01$) mRNA levels, compared with sham control treatment. VCAM-1 mRNA appeared at a level 3 times greater in the sham control than in the irradiated arteries at 1 day after treatments. In the contrast, Figure 13 showed the expression of VCAM-1 in porcine LAD and RCA. We studied the different expression pattern between LAD and RCA in different treatments. Surprisingly the expression of

VCAM-1 of RCA was 2 folds higher than that of LAD in Re188, PTCA/Re, and Re/PTCA groups. Irradiation at the 20 Gy dose induced a significant increase at the mRNA levels of VCAM-1 of RCA ($p < 0.01$), all compared with VCAM-1 of LAD. In contrast, the expression of VCAM-1 of RCA was lower than that of LAD in PTCA group. Balloon-overstretch injury induced a significant decrease at the mRNA levels of VCAM-1 of RCA ($p < 0.05$), all compared with VCAM-1 of LAD. In contrast, the expression of VCAM-1 of RCA slightly increased, despite the lack of an earlier significant difference from that of LAD in the sham control group. Otherwise no matter which coronary arteries we studied, the expression of VCAM-1 was higher in the sham control group than that in PTCA, Re188, PTCA/Re, and Re/PTCA groups.

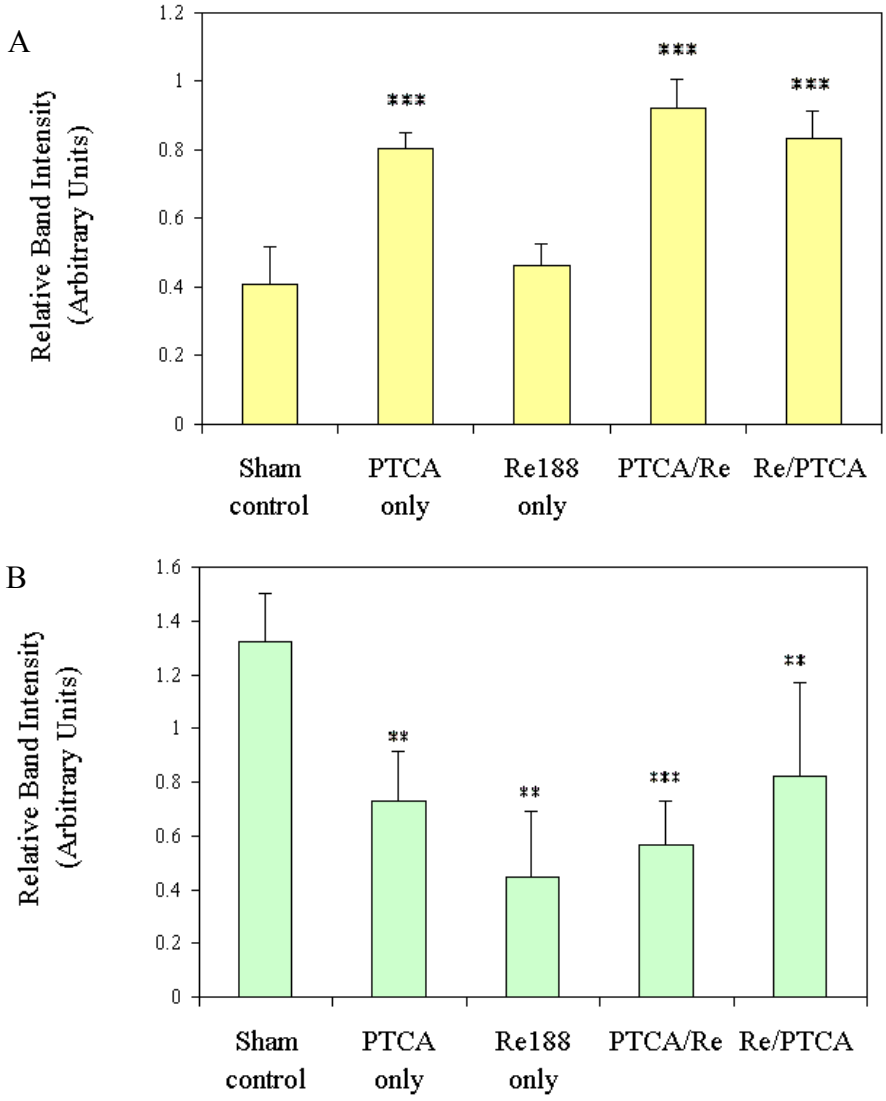

Figure 11. RT-PCR of ICAM-1 and VCAM-1 compared with GAPDH mRNA at 1 day after treatment. cDNA from the (A) ICAM-1 mRNA was amplified 28 cycles and from the (B) VCAM-1 mRNA was amplified 24 cycles. PCR products were electrophoresed in 2% agarose gels and stained with ethidium bromide (n = 4). Gels were scanned and the bands were quantified. Other treatments included PTCA, Re188, PTCA prior to Re188, and PTCA after Re188. ** $p < 0.01$ indicates significantly different from control value, and *** $p < 0.001$ indicates significantly different from control value. Yellow color responses ICAM-1 and green color responses VCAM-1.

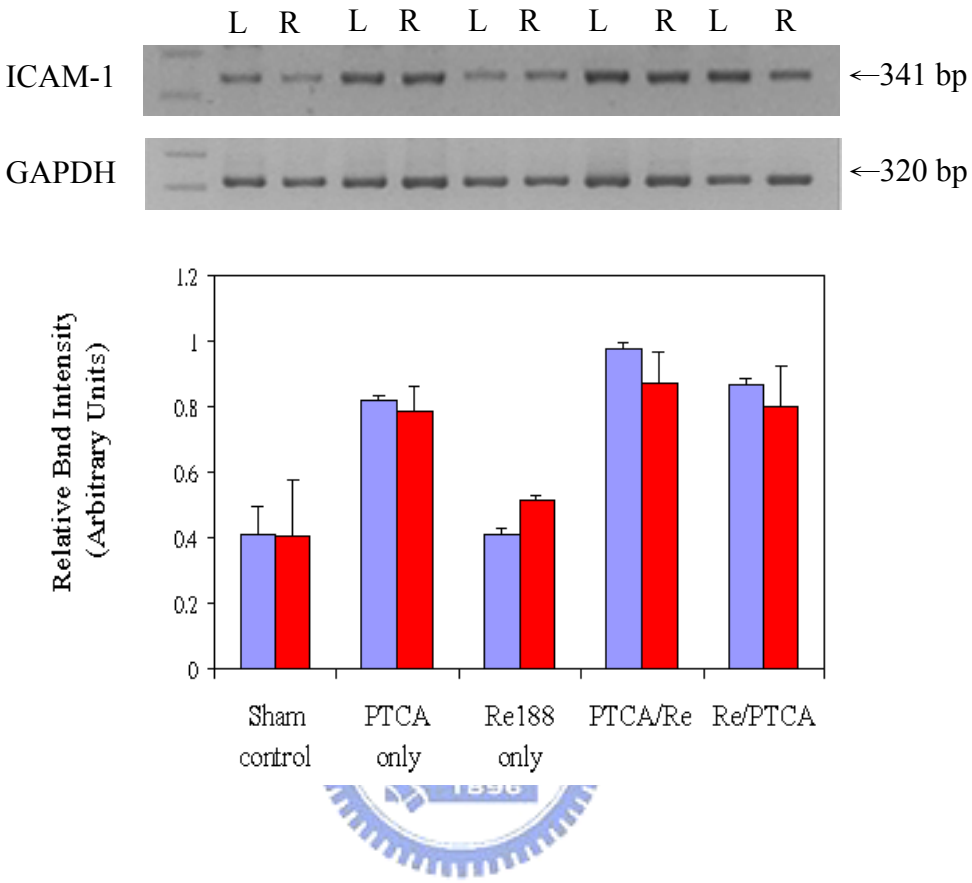

Figure 12. RT-PCR of ICAM-1 compared with GAPDH mRNA in LAD and RCA at 1 day after treatments. cDNA from the ICAM-1 mRNA was amplified 28 cycles (n = 2). The treatments included PTCA, Re188, PTCA prior to Re188, and PTCA after Re188. Lane L indicates LAD. Lane R indicates RCA. The expression of ICAM-1 in response to radiation was similar to that in sham control group. The expression value between LAD and RCA is not significant (NS). Blue color responses LAD and red responses RCA.

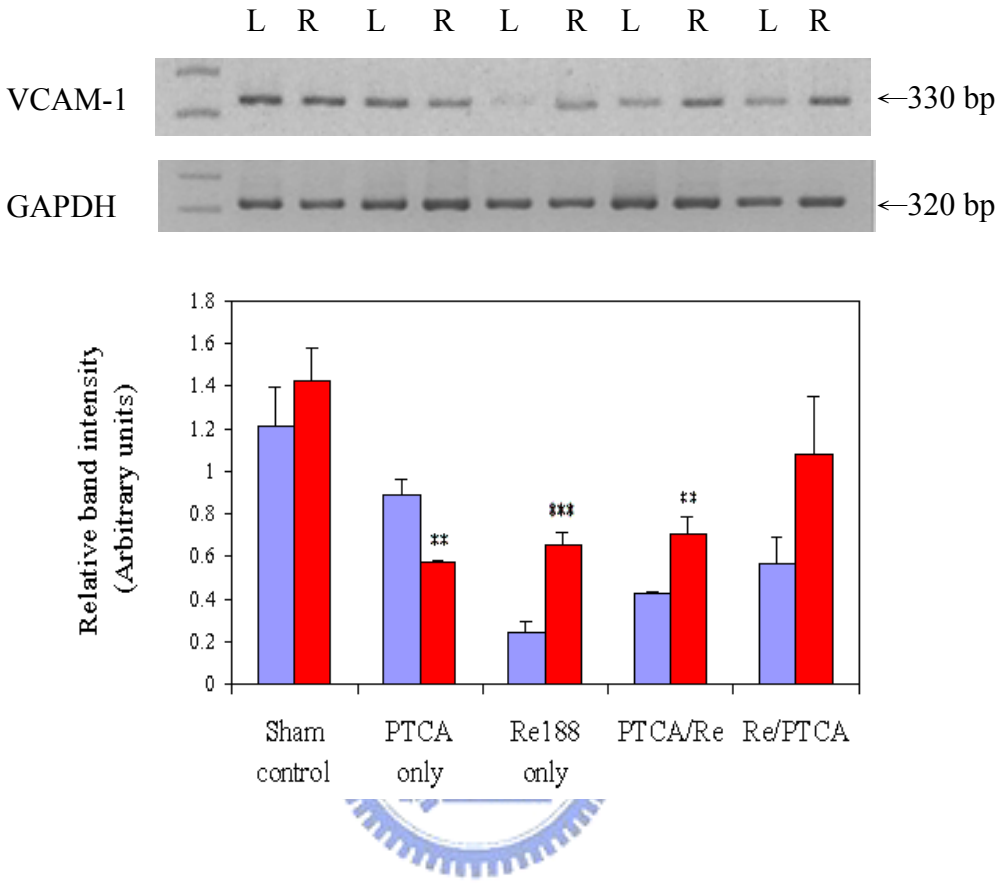

Figure 13. RT-PCR of VCAM-1 compared with GAPDH mRNA in LAD and RCA at 1 day after treatments. cDNA from the VCAM-1 mRNA was amplified 24 cycles (n = 2). PCR products were electrophoresed in 2% agarose gels and stained with ethidium bromide. Lane L indicates LAD. Lane R indicates RCA. The treatments include PTCA, Re188, PTCA prior to Re188, and PTCA after Re188. ** $p < 0.01$ indicates significantly different between LAD and RCA in the same treatment, and *** $p < 0.001$ indicates significantly different between LAD and RCA in the same treatment.

3. mRNA expression levels of NF-κB exposure to γ-radiation in vitro

Using semiquantitative RT-PCR the cycle numbers for GAPDH and NF-κB in the samples was fixed at 20 and 28 cycles respectively. Their expression levels on VSMC were estimated and plotted (data not shown).

To study the influence of transcription factor of ionizing radiation on VSMCs, the mRNA level of NF-κB was evaluated 3 days after radiation of 2 Gy and 20 Gy. In precious studies, NF-κB can be activated by radiation. In Figure 14 the expression of NF-κB decreased significantly as expected at 1 day post-radiation. The expression of NF-κB with untreated cultured of cells was 4 folds greater than that with radiated cells at 1 day after radiation. On the contrary, the expression of NF-κB on radiated VSMCs showed constant increase at 2 and 3 day post-irradiation. The expression of NF-κB increased 3 folds following radiation (2 Gy) at 2 day and 3 day, compared with that on the first day. When 20 Gy was applied on VSMCs and observed for 3 days, the expression of NF-κB was no significantly different (data not shown) between nonirradiated and radiated VSMCs.

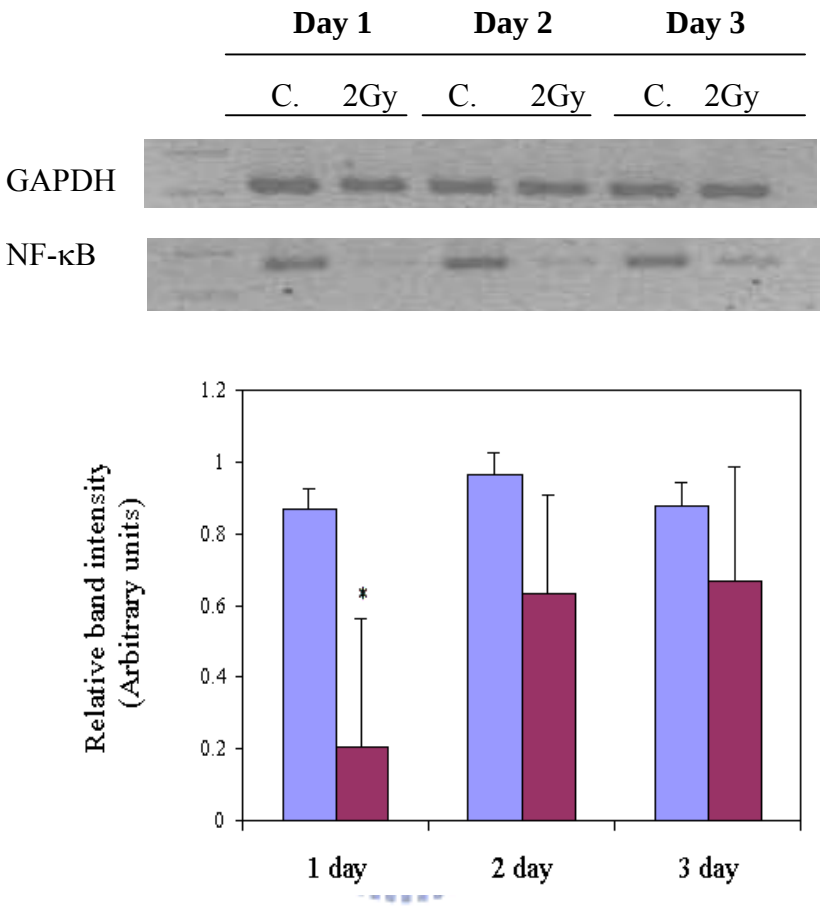

Figure 14. NF-κB compared with GAPDH mRNA on nonirradiated VSMC and on radiated cells at 1, 2, and 3 day following γ-radiation. From the graph it was obvious that NF-κB expression increased at 2 day and stably increased at 3 day following radiation (n = 3). * indicates that is significantly different from the nonirradiated cells as determined by t test at $p < 0.05$. Blue color bar indicates nonirradiated cells and brown color indicates 2 Gy-radiated cells at 1, 2, and 3 day post-irradiation